JOURNAL OF BACTERIOLOGY, May 2001, p. 2918–2928 Vol. 183, No. 9
0021-9193/01/$04.00+0 DOI: 10.1128/JB.183.9.2918–2928.2001

Mapping Stress-Induced Changes in Autoinducer AI-2 Production in Chemostat-Cultivated *Escherichia coli* K-12

MATTHEW P. DELISA,[1,2] JAMES J. VALDES,[3] AND WILLIAM E. BENTLEY[1,2]*

Center for Agricultural Biotechnology, University of Maryland Biotechnology Institute,[1] and Department of Chemical Engineering,[2] University of Maryland, College Park, Maryland 20742, and U.S. Army Edgewood Chemical Biological Center, Aberdeen Proving Ground, Maryland 21010[3]

Received 8 November 2000/Accepted 6 February 2001

Numerous gram-negative bacteria employ a cell-to-cell signaling mechanism, termed quorum sensing, for controlling gene expression in response to population density. Recently, this phenomenon has been discovered in *Escherichia coli*, and while pathogenic *E. coli* utilize quorum sensing to regulate pathogenesis (i.e., expression of virulence genes), the role of quorum sensing in nonpathogenic *E. coli* is less clear, and in particular, there is no information regarding the role of quorum sensing during the overexpression of recombinant proteins. The production of autoinducer AI-2, a signaling molecule employed by *E. coli* for intercellular communication, was studied in *E. coli* W3110 chemostat cultures using a *Vibrio harveyi* AI-2 reporter assay (M. G. Surrette and B. L. Bassler, Proc. Natl. Acad. Sci. USA 95:7046–7050, 1998). Chemostat cultures enabled a study of AI-2 regulation through steady-state and transient responses to a variety of environmental stimuli. Results demonstrated that AI-2 levels increased with the steady-state culture growth rate. In addition, AI-2 increased following pulsed addition of glucose, Fe(III), NaCl, and dithiothreitol and decreased following aerobiosis, amino acid starvation, and isopropyl-β-D-thiogalactopyranoside-induced expression of human interleukin-2 (hIL-2). In general, the AI-2 responses to several perturbations were indicative of a shift in metabolic activity or state of the cells induced by the individual stress. Because of our interest in the expression of heterologous proteins in *E. coli*, the transcription of four quorum-regulated genes and 20 stress genes was mapped during the transient response to induced expression of hIL-2. Significant regulatory overlap was revealed among several stress and starvation genes and known quorum-sensing genes.

Synthesis and perception of a self-produced, freely diffusible signal molecule, termed autoinducer AI-2, by the gram-negative bacterium *Escherichia coli* is thought to regulate the expression of a variety of genes in response to population density. This process, termed autoinduction or quorum sensing, was first described in *Vibrio fischeri* (39), and similar autoregulatory mechanisms have since been reported in a wide range of bacteria, including *Pseudomonas aeruginosa* (34), *Erwinia carotovora* (5), and *Agrobacterium tumefaciens* (40), as well as *E. coli* (18, 44, 57). Although the existence of such a mechanism in *E. coli* has been uncovered, the genetic, physiological, and environmental factors that contribute to and regulate the quorum circuitry remain poorly defined.

Evidence of intercellular communication in *E. coli* came with the discovery of a quorum-regulated transcriptional *trans*-activator (SdiA) of the cell division genes in the *ftsQAZ* locus homologous to LuxR of *V. fischeri* (18, 44, 57) and a synthase protein ($LuxS_{E.c.}$) responsible for AI-2 signal molecule production (49). Further elucidation of native *E. coli* quorum circuit architecture resulted from the *Vibrio harveyi* cross-species activity assay of Surette and Bassler (47), which has greatly facilitated autoinduction research in faculative anaerobes (46, 47). This is particularly important as much of the information pertaining to the regulatory machinery controlling quorum-dependent gene expression in *E. coli* had previously been derived from studies of *E. coli* cloned with *V. fischeri lux* genes or indirectly from cognate studies of *V. fischeri* (53). It has already been shown that AI-2-stimulated quorum sensing in *E. coli* is critical for regulating behavior during prestationary growth and that AI-2 communicates cell density, growth rate, glucose level, and metabolic potential of the environment (47, 48). Moreover, regulation of AI-2 in *E. coli* appears to be utilized for channeling conditions of stress and starvation into the quorum circuit, presumably through the GroESL chaperonin complex (12, 48, 53). In particular, a factor present in *E. coli*-conditioned medium (CM) stimulates expression of *rpoS, sdiA*, and the *ftsQAZ* cell division cluster (18, 44) and inhibits chromosomal replication (58), suggesting intimate involvement of the quorum circuit with stress- and starvation-mediated and cell cycle circuits in *E. coli*.

Still, autoinduction in *E. coli* remains enigmatic, as the signaling molecule, the precise mechanism of signaling, and the cellular and environmental stimuli involved in global AI-2 regulation are poorly defined. It is known that a variety of environmental cues play a role in regulating *lux* expression in *E. coli*, but a systematic study of the effect of these stimuli on the native quorum circuit in *E. coli* (i.e., AI-2 regulation) is lacking. Further, it is difficult to uncouple population density-dependent effects from growth phase effects in batch culture, making it unclear whether patterns of AI-2 regulation are population density or growth phase effects. In the present study, we assayed AI-2 production in continuous culture (41) to explore various transients commonly observed during fermentation processes, including physical and chemical insults, as well as the induction of heterologous protein. For example, growth of

* Corresponding author. Mailing address: Center for Agricultural Biotechnology, University of Maryland Biotechnology Institute, University of Maryland, College Park, MD 20742. Phone: (301) 405-4321. Fax: (301) 314-9075. E-mail: bentley@eng.umd.edu.

E. coli is often regulated by transient substrate and nutrient limitations, oxygen transfer capabilities, formation of growth-inhibitory by-products, and limitations in heat dissipation (36). Also, the act of producing recombinant proteins elicits stress responses (2, 22, 24, 25, 33). Chemostat cultivation offered a reproducible, regulated growth environment so that regulation of AI-2 could be isolated from continuously changing variables, such as oxygen, glucose, and pH, which likely obscure AI-2 regulatory phenomena in batch cultures. Therefore, we monitored dynamic AI-2 production during the transitory period between steady states caused by either dilution rate changes or induced perturbations (i.e., heat shock and ethanol stress) to steady-state cultures of recombinant *E. coli*. Results presented here show that shifts in intracellular metabolism and stress resulted in significantly altered patterns of AI-2 accumulation, demonstrating that AI-2 production is a complex function of environmental and intracellular conditions.

Our ultimate objective is to better understand the communication between *E. coli* during fermentation processes in order to facilitate expression of heterologous genes. Importantly, little is known about the attenuated induction of heterologous proteins commonly observed at high cell densities (11, 19, 50), where factors such as decreased growth rate, increased cell death, increased lysis, decreased metabolic activity, and segregation into viable but nonculturable cells can negatively impact reactor productivity (2, 28, 43). We have shown dramatically altered transcript levels of several stress-related genes at cell densities near 80 g (dry weight) liter^{-1} (20), and recent understanding of autoinduction suggests possible mechanisms that contribute to the altered metabolic and physiological state of cells grown to these cell densities. In this work, we have also explored the transcriptional response of 24 genes, including four known quorum-related genes as well as a known subset of genes up-regulated in response to human interleukin-2 (hIL-2) production, in order to begin mapping quorum-dependent transcriptional regulation with bacterial stress responses.

MATERIALS AND METHODS

Bacterial strains, plasmids, and culture media. *E. coli* K-12 strain W3110, harboring the plasmid phIL-2 for hIL-2 protein (9) or strain MDAI2 (W3110 *luxS*::Tc^r) bearing plasmid pGFPuv-*ftsQ2p* for measuring SdiA-mediated *ftsQA* transcription was used in this study (M. P. DeLisa, J. J. Valdes, and W. E. Bentley, submitted for publication). *V. harveyi* strains BB170 (*luxN*::Tn*5* sensor 1$^-$ sensor 2$^+$) and BB152 (*luxL*::Tn*5* A1-1$^-$ AI-2$^+$) were used for *E. coli* autoinducer activity assays and were kindly provided by B. L. Bassler. Luria-Bertani (LB) medium contained yeast extract (5 g liter^{-1}; Sigma Chemical Co.), Bacto Tryptone (10 g liter^{-1}; Difco), and NaCl (10 g liter^{-1}) and was supplemented with 5 mM glucose, unless noted otherwise. Autoinducer bioassay (AB) and LM media are described in detail elsewhere (6, 26).

Chemostat experiments. Temperature- and pH-regulated microfermentors (56) specifically designed for long-term continuous cultivation were inoculated with 1% (vol/vol) overnight LB cultures and maintained at pH 6.7 and 30°C with 225-rpm agitation. All chemostat experiments were either sparged with air (200 ml min^{-1}) or unsparged but vented as noted. For continuous culture, a steady state was defined by unchanged optical density at 600 nm (OD_{600}) for a period of 5 to 6 residence times. Dilution rate changes were implemented by altering the feed rate of fresh LB medium to the reactor. At steady state, the dilution rate is equivalent to the growth rate of the culture (41). Experimental data associated with a particular dilution rate (or transition between dilution rates) are the averages of three samples each assayed in triplicate using BB170 ($n = 9$), and all data are the averages of duplicate experiments.

Intracellular and environmental stimuli. Physical or chemical insults were applied to steady-state *E. coli* cells ($\mu = 0.75$ h^{-1}) and 2-ml samples were drawn over a 4-h period (ca. 3 residence times), allowing dynamic measurement of the AI-2 response. Specifically, glucose, which has previously been implicated in AI-2 regulation (14, 38, 47), was pulse fed (ca. 50 mM) to steady-state cultures. The effect of iron, known to delay the onset of luminescence in *V. fischeri* (13), was investigated by pulse addition of ferric [Fe(III)] citrate (100 mg liter^{-1}). High osmolarity has been shown to stimulate AI-2 production in *Salmonella enterica* serovar Typhimurium (48) and thus was investigated by addition of NaCl (35 g liter^{-1}). Increased aerobiosis was investigated by delivery of oxygen (200 ml min^{-1}) to the fermentor. Heat shock was induced by temperature elevation of the reactor jacket from 30 to 42°C, which resulted in culture temperature change over 5 min. Ethanol, which elicits a stress response similar to heat shock (55), was pulse added (4% [vol/vol]). Stringent stress was induced via serine hydroxamate addition (42). Oxidative stress was generated by addition of hydrogen peroxide (54) or by addition of dithiothreitol (DTT) (a membrane-permeating reducing agent) to a final concentration of 1 g liter^{-1} (21). The presence of acetate has been linked to low productivity in recombinant *E. coli* cultures (31) and was investigated by addition of 6 g of sodium acetate per liter. Finally, the expression of recombinant hIL-2 was induced by addition of 1 mM isopropyl β-D-thiogalactopyranoside (IPTG) (Sigma).

Analytical methods. Cell growth was monitored by measuring OD_{600} with a UV-visible light spectrophotometer (Beckman DU 640). To determine glucose concentration, 1-ml whole broth samples were centrifuged (10,000 × *g* at 4°C) and glucose concentration of the supernatant was measured using a glucose analyzer (YSI Model 2700). Green fluorescent protein (GFP) was assayed in whole cells as previously reported (8), and readings were made using a Perkin-Elmer LS-3B fluorescence spectrometer at an excitation wavelength of 395 nm and an emission wavelength of 509 nm. Specific fluorescence intensity was obtained by normalizing relative fluorescence intensity of samples by OD_{600} of the sample.

Preparation of cell culture fluids and CM. Cell culture fluids were prepared by centrifugation of 2-ml *E. coli* whole-broth samples for 5 min (10,000 × *g* at 4°C). Cleared supernatants were passed through 0.2-μm-pore-size HT Tuffryn filters (Pall Corp) and stored at −20°C. *V. harveyi* BB152 cell culture fluids were prepared likewise to obtain positive control samples as reported previously (47). CM was prepared by growing W3110 or MDAI2 in LB–50 mM glucose to an OD_{600} of 2 to 3 (~6 to 8 h) followed by centrifugation (5 min, 10,000 × *g* at 4°C) and filtering of cleared supernatants as above.

Autoinducer activity assay. *E. coli* cell culture fluids were tested for the presence of AI-2 using the *V. harveyi* reporter strain BB170, which responds only to AI-2 (47). Luminescence assays were performed as outlined elsewhere (47) and luminescence was measured as a function of *V. harveyi* cell density by quantitating light production with a luminometer (EG&G Berthold). Data reported as fold activation were obtained by dividing the light produced by the reporter after addition of *E. coli* culture fluid by the light output of the reporter when growth medium alone was added. Importantly, for quantification of AI-2 activity level, a detailed standard curve of CM samples serially diluted in fresh AB medium (25-fold difference in CM volume) was utilized to demonstrate concentration dependence of the assay. The resulting standard curve had an r^2 of 0.9, and all CM samples outside the linear range were diluted appropriately in AB medium.

RNA isolation and total RNA dot blotting. Whole-cell samples (1 ml) were immediately flash frozen in liquid nitrogen and stored at −80°C. RNA purification was carried out using the RNAqueous total RNA isolation kit (Ambion). This kit typically purified 10 μg of total RNA per ml of *E. coli* culture at an OD_{600} equivalent of 1.0.

Total RNA dot blots were performed by pipetting 1 to 5-μg total RNA samples (in 50% formamide, 6.5% formaldehyde, and 1X SSC [1X SSC is 0.15 M NaCl plus 0.015 M sodium citrate]) onto nylon membranes using a Schleicher and Schuell microsample filtration manifold. Fixing of nylon membranes was performed via UV-induced cross-linking. Membranes were prehybridized for 1 h in 15 ml of hybridization buffer (Boehringer Mannheim). Prehybridization solution was decanted, and 7.5 ml of fresh hybridization buffer containing 50 ng of digoxigenin (DIG)-labeled Northern probe ml^{-1} was introduced. Northern probes were prepared using a PCR DIG Probe Synthesis kit (Boehringer Mannheim), 25-bp oligonucleotide primers (Gene Probe Technology), and *E. coli* K-12 template DNA isolated according to the method in reference 23, and resulting probes were approximately 400 bp in length. Hybridization was carried out overnight at 50°C followed by development utilizing anti-DIG alkaline phosphatase (Boehringer Mannheim) and CSPD chemiluminescent substrate (Boehringer Mannheim) according to DIG development protocols (Boehringer Mannheim). Developed membranes were incubated at 37°C for 30 min prior to X-ray film exposure for 2 h.

Signal quantification and calculation of correlation coefficients. For quantification of total RNA dot blots, a detailed standard curve of serially diluted

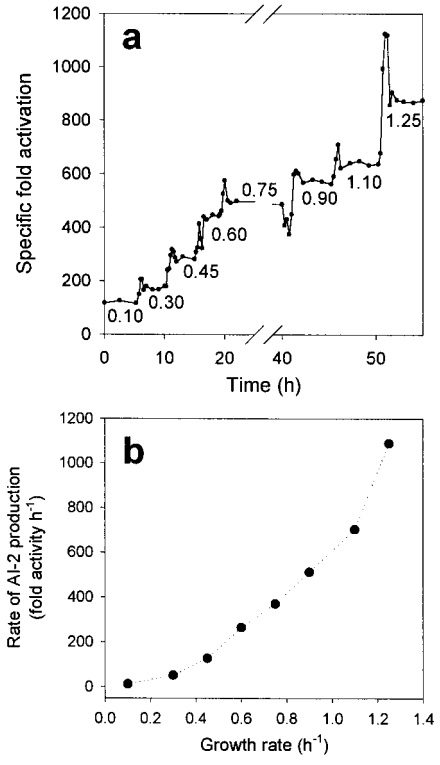

FIG. 1. AI-2 activity (a) and rate of AI-2 production (b) during steady-state transitions achieved by incremental upshift in culture growth rate (from 0.10 to 1.25 h^{-1}) of W3110/phIL-2 chemostat cultures. The AI-2 production rate is the activity times the dilution rate, D (D = reactor volume/flow rate). Steady state was achieved in ca. 3 to 5 residence times. Increased growth rate was implemented by increasing the feed rate of fresh LB medium–50 mM glucose. Replicate samples agreed within 15%.

DIG-labeled λDNA was utilized. The dilution spanned a 50-fold difference in mass of DNA per dot, and the resulting standard curve had an r^2 of 0.9. Densitometric scanning was performed for signal analysis. Images of exposed films were acquired via an EAGLE EYE II (Stratagene) image acquisition system. Image quantification was performed using Scion Image software (Scion Corporation). Lastly, induction ratios (IR) based on the density of each dot were calculated by the following equation: IR = (density/μg of RNA)$_{t=i}$/(density/μg of RNA)$_{t=0}$, and induction ratios from repeated experiments were averaged, with the standard error calculated as the standard deviation (σ) of the mean [$\sigma/(n)^{0.5}$]. The standard error ranged between 8 and 37%. Correlation among genes in response to IPTG-induced hIL-2 expression was calculated as follows: $r = \sigma_{xy}/\sigma_x\sigma_y$, where σ_{xy} is the covariance between samples x and y and σ_{xy} and σ_{xy} are the standard deviations within samples x and y, respectively (51). Determination of the probability (P) that the r value (correlation coefficient) obtained could have been calculated from uncorrelated samples is made such that the label "significant" was assigned to a P of <0.05 and the label "highly significant" was assigned to a P of <0.01.

RESULTS

Transient AI-2 response to increased growth rate and glucose perturbation. In this study, we used continuous cultures of *E. coli* to study AI-2 production in response to growth phase changes as well as to a number of environmental and intracellular factors. Results depicting the transient response in extracellular AI-2 levels following upshift in culture growth rate (Fig. 1a) illustrate that AI-2 signal molecule production was directly proportional to the growth rate of the bacterial culture.

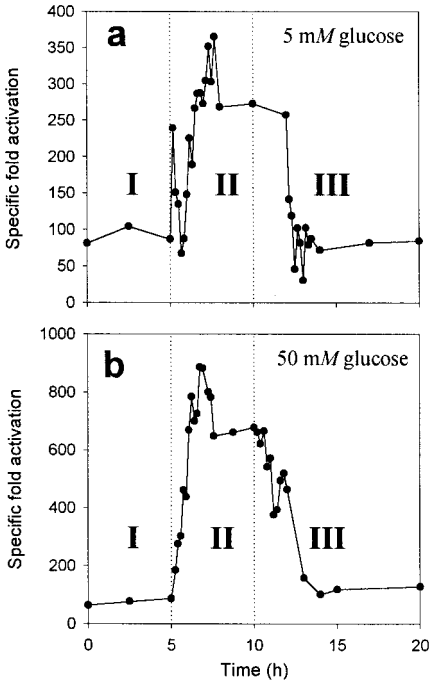

FIG. 2. AI-2 activity during transition between low growth rate (region I and III) (0.10 h^{-1}) and high growth rate (region II) (1.25 h^{-1}) of W3110/phIL-2 cultures grown in the presence of 5 (a) and 50 (b) mM glucose. Replicate samples agreed within 15%.

As the growth rate of the culture was incrementally increased from a growth rate of 0.10 to 1.25 h^{-1} (in steps of ca. 0.15 to 0.20 h^{-1}), a concomitant increase in the fold activation of AI-2 was observed. The changes in glucose concentration and cell density (OD_{600}) over this range were less than 17 and 14%, respectively (not shown). The increase in AI-2 activity from one steady state to the next was accompanied by a sharp overshoot during a transitory period prior to settling at a new steady-state AI-2 level. This observed overshoot was seen to increase in conjunction with increasing growth rate, with the largest overshoot occurring during the transition to the highest growth rate evaluated (1.10 to 1.25 h^{-1}). In addition, the rate of AI-2 production was seen to increase with increasing growth rate (Fig. 1b). To help distinguish between the effect of glucose levels and growth rate, we performed chemostat experiments for which W3110/phIL-2 cells were grown in the absence of glucose. Importantly, results for growth of W3110/phIL-2 cells in LB medium without glucose demonstrated similarly that the increase of AI-2 with increasing culture growth rate occurred, but at a lower overall level for each growth rate compared to cells grown in 50 mM glucose (not shown). Therefore, glucose affected only the relative magnitude of AI-2 but was not required for AI-2 production under the conditions studied. The phenomenon of increasing AI-2 with increasing growth rate was approximately linear for growth rates between 0.45 and 1.10 h^{-1} but was visibly nonlinear for growth rates below 0.45 and above 1.10 h^{-1}. Interestingly, manifestation of this nonlinearity, which was seen as an equivalent shift in growth rate (0.10 to 1.25 h^{-1}), when made in one step, resulted in a smaller increase in AI-2 level after the final steady state was achieved

(Fig. 2b). The transition, however, was completely reversible, as both AI-2 and OD_{600} returned to the initial state after the dilution rate was dropped back to the initial value (0.10 h^{-1}).

As glucose concentration has also been shown to affect AI-2 activity in *E. coli* (47), the transient response following upshift in culture growth rate in the presence of differing glucose levels (Fig. 2) was found to be influenced by the feed glucose concentration. That is, in Fig. 1, AI-2 activity increased ca. 10-fold as the growth rate was incrementally increased (0.10 to 1.25 h^{-1}) in medium supplemented with 50 mM glucose. In Fig. 2a and b, a one-step increase in growth rate (0.10-1.25 h^{-1}) resulted in ca. 2.5- and 6.3-fold increase in AI-2 activity in the presence of 5 and 50 mM glucose, respectively. Interestingly, in the presence of a higher glucose concentration (50 mM) and a one-step upshift (Fig. 2b), increasing the growth rate led to 2.5 times more AI-2 activity compared to that observed for cells grown in the presence of a lower glucose concentration (5 mM) (Fig. 2a) but was ca. 1.6 times lower than AI-2 activity produced by increasing the growth rate in 0.10 h^{-1} steps (Fig. 1 versus Fig. 2b). In all cases, transition to a higher growth rate resulted in overshoot of the AI-2 activity during the 2.5-h transitory period (region II) prior to reaching the new steady-state level. Decreasing the culture growth rate back to 0.10 h^{-1} (region III) resulted in AI-2 activity equal to the original steady-state levels. The time required to reach steady state during this downshift was ca. 4.5 h (compared to 2.5 h during upshift).

Glucose-induced perturbations from steady state stimulate AI-2 production. We next perturbed steady-state W3110/phIL-2 cultures grown in LB medium–5 mM glucose with a glucose spike (50 mM pulse fed to reactor). Both cases (μ = 0.75 and 0.10 h^{-1}) exhibited a relatively rapid upswing followed by decline back to the preperturbed level. However, unlike other perturbations studied, a second peak in AI-2 activity was observed as the glucose concentration fell below ca. 10 mM due to consumption and washout. This response was likely triggered by a decline of glucose concentration below a threshold level, consistent with previous batch experiments (47, 48) that show a spike in AI-2 activity concomitant with glucose depletion. As expected based on prevailing glucose consumption rates, the time required for the entire glucose response was much shorter for the higher growth rate case (not shown), but normalizing the perturbation time demonstrates that the AI-2 responses were similar (Fig. 3). That is, the elapsed time was normalized by dividing the time postperturbation by the time at which the glucose had reached 8% of its peak (ca. 40 to 45 mM) value, a fixed point common to both chemostat experiments. Notably, comparing Fig. 3a and b reveals that the fold activation of AI-2 signal activity in response to pulsed glucose was almost 2 times greater at the higher growth rate versus the fold AI-2 activation at the lower growth rate.

Intracellular and environmental stimuli perturb AI-2 signal. Since several environmental cues are known to affect *lux* gene expression in *V. fischeri* or in *E. coli* (via plasmid-borne *lux* genes), we investigated the effect of these stimuli on AI-2 activity in steady-state chemostat cultures of W3110/phIL-2 grown in LB medium–5 mM glucose. Specifically, pulse addition of several stimuli (see Materials and Methods) to steady-state cultures (maintained at μ = 0.75 h^{-1}) was performed and

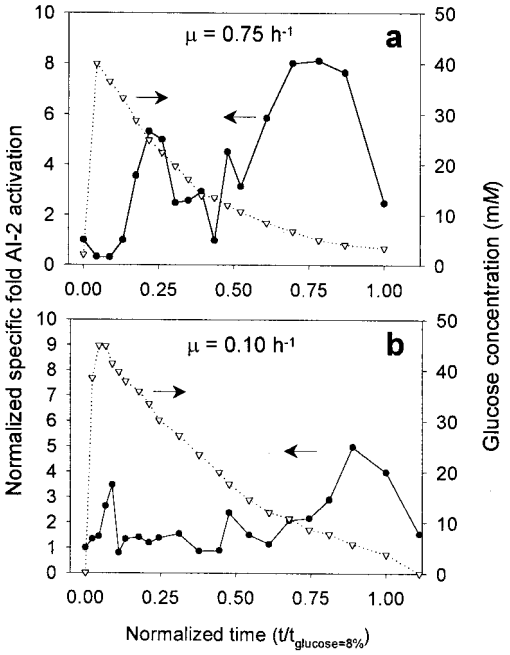

FIG. 3. AI-2 activity (closed circles) following glucose-induced perturbation from steady state in cultures of W3110/phIL-2 grown at high dilution rate (0.75 h^{-1}) (a) and low dilution rate (0.10 h^{-1}) (b). Data are reported as the AI-2 activity of the sample divided by the OD_{600} of the sample, and time was normalized by dividing the time postperturbation by the time at which the glucose had reached 8% of its peak value, which was a fixed point common to both chemostat experiments ($t_{8\%,\ D\ =\ 0.75}$ = 240 min; $t_{8\%,\ D\ =\ 0.1}$ = 450 min). Glucose concentration is depicted by the open triangles. Replicate samples agreed within 15%.

AI-2 activity was monitored at high frequency for the subsequent 4 h (i.e., 3 residence times) (Fig. 4). Superimposed onto these responses (Fig. 4a [iron pulse] and [hIL-2 expression]) is the theoretical concentration (normalized) of a pulse-added, nonmetabolized tracer, illustrating in some cases the transient intensity of the stimulus.

Responses to increased iron [100 mg of Fe(III) citrate liter^{-1}], increased osmolarity (35 g liter^{-1}), and decreased culture redox potential (1 g of DTT liter^{-1}) exhibited AI-2 accumulation within the first 60 min that remained elevated for 3 h before returning to approximately the original steady-state level (Fig. 4a). Notably, exposure to iron resulted in the largest (ca. 3.5-fold) and most rapid (ca. 30 min) transient AI-2 increase. Additionally, a feed of LB–50 mM glucose–100 mg of Fe(III) citrate liter^{-1} resulted in ~2.5-fold increase in AI-2 activity (compared to cultures fed LB–50 mM glucose only [not shown]) over 5 residence times, confirming that the pulse-induced response was dependent upon iron concentration experienced by cells. Exposure to sodium acetate (6 g of sodium acetate liter^{-1}) resulted in an immediate decrease of AI-2 for 60 min followed by a sharp and reproducible 1.5-fold increase at 80 min, remaining elevated for 80 min before finally falling below the original steady-state level. Finally, exposure to increased oxygen (pulse input of pure O_2 [200 ml min^{-1}]) resulted in immediate decrease of AI-2 activity that persisted for 120 min. At this point, the oxygen supply to the reactor was ceased, and an immediate increase in AI-2 activity to ca. 1.5-

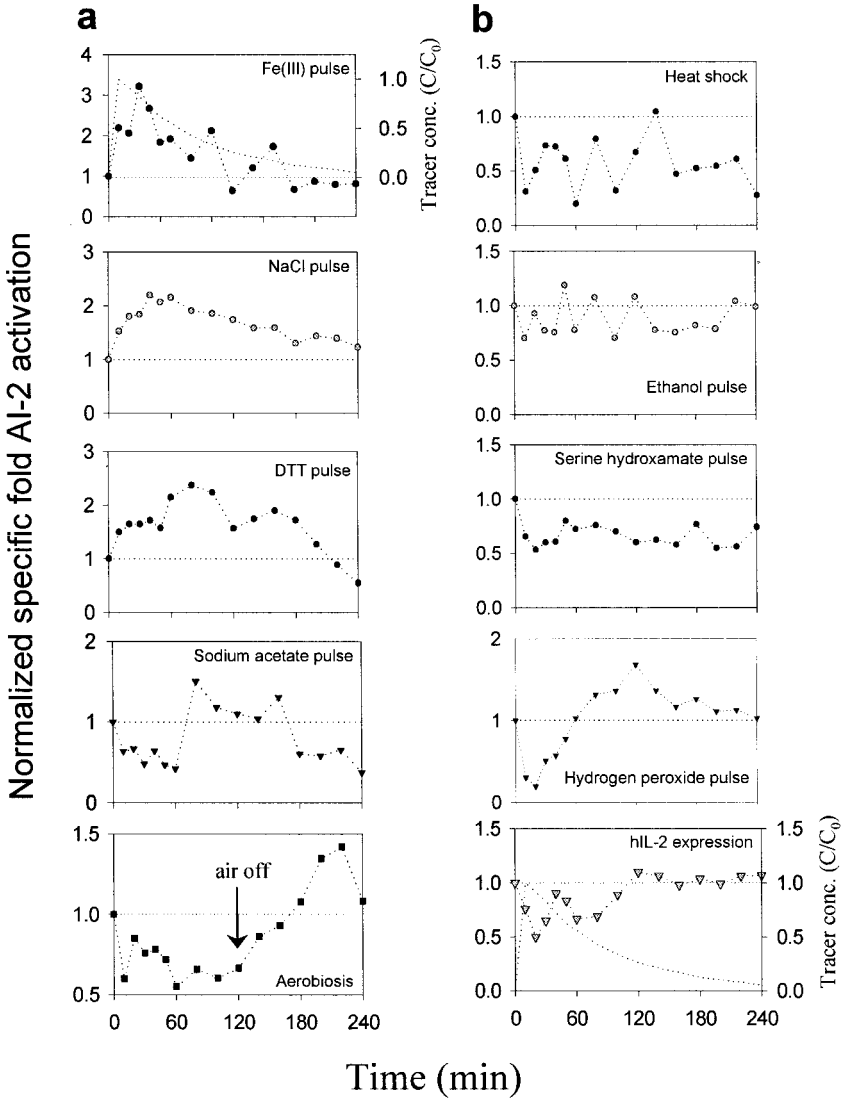

FIG. 4. AI-2 activity in response to various stimuli-induced (environmental) perturbations (a) and stress-related (intracellular and environmental) perturbations (b) of steady-state W3110/phIL-2 cultures. Data are reported as the AI-2 activity of the sample divided by the OD_{600} of the sample and normalized to the steady-state level of AI-2 activity attained prior to stimulation ($t = 0$ min). Replicate samples agreed within 15%.

fold ensued before settling back towards the steady-state level. An identical experiment was performed where oxygen was supplied over the entire 4-h period and the AI-2 activity remained low over the entire period (not shown).

The *rpoH*-mediated stresses heat shock (42°C; change in temperature, 12°C; change in time, 4 h) and ethanol (4% [vol/vol]) both resulted in decreased AI-2 production for ca. 60 min followed by an oscillatory response before reaching a steady state (Fig. 4b). In the case of heat shock, the AI-2 activity remained well below the prestress level as the reactor temperature was maintained at 42°C for the entire 4-h period. The final AI-2 level in response to ethanol (which was transiently depleted) returned to the prestress level. Interestingly, pulse addition of serine hydroxamate (100 mg liter^{-1}), known to stimulate a stringent response (42), resulted in down-regulation of AI-2 that persisted over the entire 4-h period, even after the serine hydroxamate was washed out of the reactor. Exposure to hydrogen peroxide (2 mM), known to induce oxidative stress (54), was observed to negatively regulate AI-2 production over the first 30 min; however, an increase in AI-2 production occurred over the next 100 min, reaching a peak level of 1.5-fold before settling back to the prestress steady-state level. Lastly, the effect of recombinant hIL-2 formation was investigated by addition of 1 mM IPTG. AI-2 production decreased initially but returned to the prestress level in a damped oscillatory manner. Also interesting is the observation of increased AI-2 degradation (or inhibition) poststress. That is, because AI-2 activity decreased faster than the predicted washout of AI-2 in the absence of continued synthesis, the AI-2 was either degraded or inhibited by a secreted factor, as in the cases depicted in Fig. 4b. Importantly, negative controls were performed by addition of each perturbation agent directly to CM following removal of *E. coli* cells and screened using BB170. In all cases, no measurable change in luminescence was

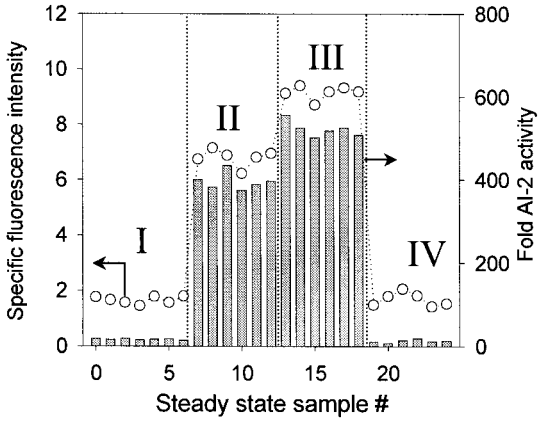

FIG. 5. SdiA-mediated activation of *ftsQA* via the *p2* promoter in chemostat culture of MDAI2/pGFPuv-*ftsQ2p* ($\mu = 0.75\ h^{-1}$). Region I feed, LB–50 mM glucose–1% Casamino Acids; region II feed, W3110 CM (AI-2 activity = 560-fold)–50 mM glucose–1% Casamino Acids; region III feed, W3110 CM (AI-2 activity = 830-fold)–50 mM glucose–1% Casamino Acids; and region IV feed, MDAI2 CM (AI-2 activity = 5-fold)–50 mM glucose–1% Casamino Acids. The condition of steady state between feed regions was achieved after ~5 residence times. Specific activity was determined as the relative fluorescence intensity of GFP-expressing whole cells normalized by the OD_{600} of the sample.

observed in the reporter strain. Additional negative controls were run by adding each agent to fresh AB medium at a concentration comparable to that in steady-state samples. Results confirmed that the presence of each agent alone did not stimulate light production in the reporter strain.

AI-2 signals through SdiA in steady-state culture. We previously observed that AI-2 signals through SdiA, a LuxR-type transcriptional activator, through the *p2* promoter of the *ftsQA* cell division gene cluster in batch culture (M. P. DeLisa, J. J. Valdes, and W. E. Bentley, submitted for publication). To confirm that this observation was independent of dynamic changes in cell density, glucose consumption, and growth rate, we grew the *luxS* mutant strain MDAI2 harboring plasmid pGFPuv-*ftsQ2p* in a chemostat culture. Strain MDAI2 was unable to synthesize AI-2, but pGFPuv-*ftsQ2p* conferred the ability to express GFP in response to SdiA-mediated activation of *ftsQA*. Only a basal level of GFP was expressed at steady state (Fig. 5), coincident with almost no measurable AI-2 activity when LB–50 mM glucose–1% Casamino Acids was fed continuously to the reactor ($\mu = 0.75\ h^{-1}$ [region I]). However, introduction of CM (generated from W3110 wild-type cells grown to an OD_{600} of 2.0 in LB–50 mM glucose; AI-2 activity = 560-fold [region II]) supplemented with 50 mM glucose–1% Casamino acids resulted in an ~3-fold increase in GFP expression coincident with a 400-fold steady-state level of AI-2 activity in the extracellular chemostat medium. Note that we previously demonstrated the sensitivity and linearity of GFP as a transcriptional promotor probe (8), and a threefold increase in GFP fluorescence corresponded to a threefold increase in transcription. Feeding of CM generated identically from W3110 wild-type cells grown to an OD_{600} of 3.0 (AI-2 activity = 830-fold [region III]) and supplemented as described above resulted in a higher steady-state level of AI-2 in the reactor and a corresponding ~4-fold induction of GFP over the basal (region I) level. Finally, introduction of CM generated from the *luxS* mutant MDAI2 grown to an OD_{600} of 3.0 in LB–50 mM glucose (AI-2 activity = 5-fold [region IV]) supplemented as described above resulted in no measurable AI-2 activity in the reactor with a simultaneous return of GFP expression to the basal level observed in region I. Overall, these results confirm that AI-2 signals to SdiA in chemostat culture independent of cell density, glucose concentration, and growth rate changes.

Quorum-regulated genes respond to induced hIL-2 expression. Using a chemostat culture, it was possible to perform a biological perturbation analysis in that steady-state cells could be physically or chemically perturbed and the characteristic footprint response, either AI-2 signaling or mRNA transcription, could subsequently be mapped. An hIL-2 induction experiment was performed exactly as described in Fig. 4b, with the addition of a second 1 mM IPTG pulse at 60 min in order to prolong the expression of hIL-2 during the 4-h response period. The transcription of 24 genes, including four known quorum-related genes ($luxS_{E.c.}$, *sdiA, ftsQ*, and *ftsA*) and 20 genes previously shown to be upregulated in batch cultures following hIL-2 expression in *E. coli*, was monitored (Table 1 and Fig. 6) (20, 22). Quantified transcript levels were converted to *Z* values ($[sample_{IR} - average_{IR}]$/standard deviation) to allow magnitude-independent analysis of the dynamic response (16). Converted data were organized via a one-dimensional self-organizing map (SOM) to guide the flipping of the nodes in subsequent hierarchical trees obtained from clustering (10). Correspondingly, the output of the SOM was analyzed using the hierarchical clustering method as described in Eisen et al. (15). The most interesting cluster borne from this analysis contained 10 genes—namely, *recA, rpoS, ftsJ, groEL, dnaK, grpE, clpP, luxS, ftsQ*, and *ftsA* (correlation coefficient of 0.74; $P = 0.008$)—which were highly significantly correlated (see Materials and Methods). Three of these genes (*luxS, ftsQ*, and *ftsA*) are directly involved in AI-2-stimulated quorum sensing (49), while *rpoS* has been intimated in *E. coli* quorum sensing (30, 35, 44) and *recA* (LexA controlled) and *groEL* and *groES* (both σ^{32} controlled) are known to regulate the *V. fischeri lux* genes in recombinant *E. coli* (53). Inclusion of *rpoH* and *is5* formed a 12-gene cluster which resulted in a statistically significant correlation coefficient ($r = 0.56$; $P = 0.037$). Finally, addition of *sdiA* (whose gene product is a LuxR-type homologue) and *ompT* still resulted in a statistically significant correlation ($r = 0.52$; $P = 0.048$). To strengthen our claim that quorum sensing overlaps stress circuits, we grew several heat shock protein mutants (*groEL140, groES30, dnaK756, dnaJ259*, and *grpE280*) in chemostat cultures (LB–0.8% glucose; $\mu = 0.75\ h^{-1}$) and determined AI-2 production (Table 2). We observed that *groES* and *groEL* mutants produced a steady-state level of AI-2 approximately twofold higher than their nonmutated parent while strains mutated in *dnaK, dnaJ*, and *grpE* all produced a steady-state level of AI-2 lower than their nonmutated parent. In all cases, strains were grown under identical conditions ($\mu = 0.75\ h^{-1}$) and attained nearly identical cell densities ($OD_{600} = 1.2 \pm 0.1$), confirming that observed differences in AI-2 production between mutant and parental strains was a consequence of an altered σ^{32}-regulatory pathway.

The AI-2 response and *Z* values of the 10 most tightly

TABLE 1. Identified stress- and quorum-related genes analyzed by total RNA dot blotting

Stress- or quorum-related gene	Stress or quorum characteristic
aceA	Stationary, utilization of acetate
clpA	Heat shock, ATP-binding subunit
clpP	Heat shock, SOS, ATP-dependent proteolytic subunit
degP	Heat shock, serine protease
dnaJ	Heat shock, chaperone
dnaK	Heat shock, stationary, chaperone
ftsA	Quorum-regulated cell division
ftsH (*hflB*)	Heat shock, bacteriophage, cell growth control
ftsJ	Heat shock, cell division and growth
ftsQ	Quorum-regulated cell division
groEL	Heat shock, bacteriophage, quorum-related chaperone
groES	Heat shock, bacteriophage, quorum-related chaperone
grpE	Heat shock, growth after prophage induction
ibpA	Heat shock, inclusion body protein, chaperone
is5 transposase	Transposition
lon	Heat shock, SOS, ATP-dependent protease
luxS	Quorum-related, autoinducer synthase
ompT	Heat shock, outer membrane protease
pspA	Heat shock, bacteriophage, regulation of PSP operon
recA	SOS, bacteriophage, possible quorum regulator
rpoH	Heat shock, RNA polymerase σ^{32} subunit
rpoS	Stationary, RNA polymerase σ^{32} subunit
sdiA	Quorum-regulated, regulation of cell division *ftsQAZ* cluster
uvrB	SOS, UV resistance

clustered genes (Fig. 7a and b) and the time-dependent average of these 10 genes (Fig. 7c) show that, initially, transcript levels increased coincident with a drop in AI-2 activity (thus, they are inversely related). Between 60 and 120 min, the initial pulse of IPTG was being washed out of the reactor and the dynamic response of AI-2 and mRNA transcripts were both presumably migrating back to the approximately steady-state levels ($t = 0$ min). At 120 min, the second pulse of IPTG resulted in a more attenuated AI-2 response, in that a lag of ~40 min was observed before AI-2 declined and the magnitude of the decline was less severe than that observed following the first pulse. The transcriptional response during this period was similar, in that it was also much more attenuated, maintaining a relatively constant level for ~80 min before declining at the end of the experiment.

DISCUSSION

To date, all regulatory studies of quorum sensing have been performed in shake flask cultures, where biomass, dissolved oxygen concentration, pH, and glucose all change continuously, which can obscure quorum-dependent regulatory phenomena that are otherwise independent of these variables. Therefore, we have used a *V. harveyi* cross-species bioassay (47) and continuous culture (37, 41) to track *E. coli* quorum signaling in response to intracellular stress and/or environmental deficiencies. Specifically, we monitored transient AI-2 production by steady-state chemostat cultures of W3110/phIL-2 perturbed by either changes in dilution rate (and therefore in growth rate) or imposition of an intracellular or environmental stimulus. As noted previously by Freeman and Bassler (17), the autoinducer assay for measuring light emission is extremely simple, enabling precise quantification of light production over a wide range of magnitudes such that the effects of quite subtle perturbations of the system can be measured reliably. Chemostat culture enabled decoupling of population density and growth rate effects, enabling the demonstration that AI-2 production not only is growth rate dependent but also exhibits interesting dynamic behavior during upshifts (overshoot) and downshifts (sluggish lag) in dilution rate. Further, it was found that production of AI-2 in chemostat culture did not require glucose metabolism. More frequent sampling of identically performed batch cultures grown in the absence of glucose confirmed that infrequent sampling may have excluded discovery of this subtle feature previously (45).

Further, we confirmed that AI-2 signals to SdiA in chemostat culture independent of cell density, glucose concentration, and growth rate dynamics, suggesting a role for AI-2 signaling in *ftsQA*-dependent control of cell division. Previous reports regarding quorum-activated *ftsQA* expression from the upstream *p2* promoter have been somewhat ambiguous. Two early reports suggested that SdiA modestly regulated the expression of the cell division locus *ftsQAZ* in response to an unidentified extracellular factor (18, 44). Surette and Bassler recently reported that CM from *E. coli* 0157 and DH5α (which does not produce AI-2) had no measurable effect on β-galactosidase produced by a reporter strain (*E. coli* MC4100) harboring a *ftsQ1p2p-lacZ* fusion (48). However, fusion of both the *p1* and *p2* promoters of *ftsQA* to the *lacZ* gene may be problematic, as the *p1* promoter is *rpoS*-mediated and the promoters together demonstrate a bimodal control mechanism (44). This prevents study of the effect of AI-2 directly on the *p2* promoter as the *p1* and *p2* promoters are differentially regulated within the cell under transient growth conditions. Further support of this comes from Sitnikov and colleagues, who observed that CM induced the *p2* promoter (in $SdiA^+$ cells) approximately fivefold compared to LB controls while CM induction of the *p1* and *p2* promoters (in $SdiA^+$ cells) simultaneously resulted in only an approximately threefold change compared to LB controls (44). That is, they found increased SdiA activity in response to CM through just *p2* at a level (approximately fivefold) comparable to that which we observed (approximately fourfold maximum induction).

Finally, as we performed our experiments using CM from the same species (W3110 wild type and W3110 *luxS*::Tc^r) and in chemostat mode, where dynamic contributions were precluded, we were able to show that SdiA-mediated *p2* activation involved the extracellular AI-2 signal. We do not, however, demonstrate that AI-2 acts directly on SdiA or any other regulatory gene, yet there is existing evidence that suggests the effect is indirect. For example, detection of AI-2 in *V. harveyi* occurs via the cognate sensor LuxPQ, where LuxP is homologous to the ribose binding protein of *E. coli*. Freeman and Bassler (17) have proposed that LuxP is the primary sensor for AI-2 and that the LuxP–AI-2 complex interacts with LuxQ for transduction of the signal to an intermediary protein (LuxU) prior to activation of the response regulator (LuxO). Interestingly, Kanamaru and colleagues found that culture supernatants of *E. coli* O157:H7 bound the N-terminal portion of SdiA, and while the factor(s) was not AI-2, they proposed a dual quorum-sensing system involving AI-2 and perhaps AI-like homoserine lactone analogues might bimodally regulate the activity of SdiA (32).

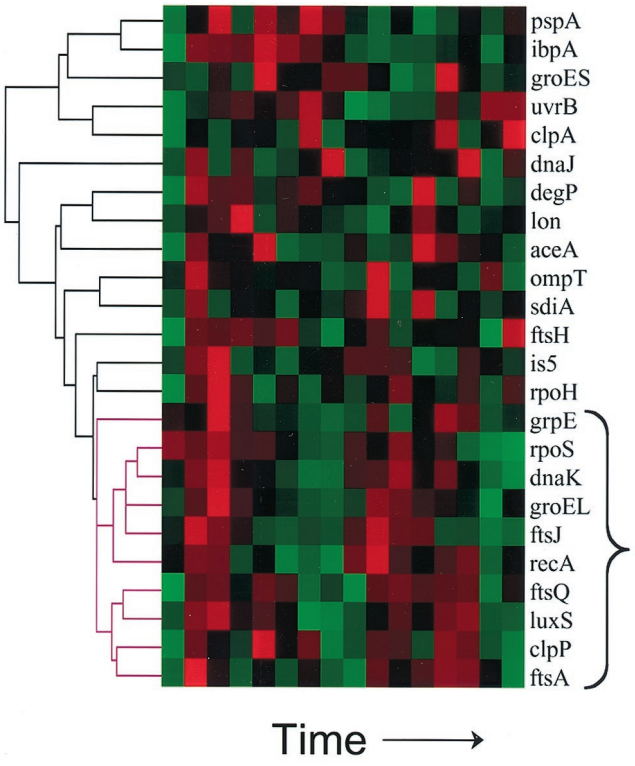

FIG. 6. Clustered display of transient data from time course of IPTG-induced cultures of steady-state W3110/phIL-2. Briefly, steady-state culture was induced with 1 mM IPTG, and samples were taken every 10 min for 1 h and every 20 min for the final 3 h (4 h total, 16 time points). The brace corresponds to genes having a correlation coefficient of 0.74. Red, up-regulation; green, down-regulation; black, constitutive.

The broad number of gram-negative bacteria which employ quorum sensing, coupled with the genetic and mechanistic similarities of their quorum systems, indicate that autoinduction is an evolutionarily conserved process used to orchestrate gene expression with population density. However, an evolving body of evidence supports the presumption that quorum sensing may play a more centralized role in bacterial physiology, with the quorum circuit confluent with stress and starvation-sensing circuits for regulating adaptation to nutritionally challenged and/or nonideal growth environments. Supporting this notion are several proposed autoinduction models that include both σ^{32}- and σ^{S}-regulated gene products as well as indirect involvement of *rpoH* and *rpoS* (1, 4, 35, 44, 45, 53). Chemostat experiments enabled a study of AI-2 signaling during transient adaptation to physical and chemical stimuli, several of which are known to induce σ^{32}- or σ^{S}-mediated responses and which were initiated by secondary phenotypic changes instead of direct gene or protein level alterations. For example, four stimuli (glucose, iron [Fe(III)], NaCl, and DTT) induced up-regulation of AI-2 activity independent of population density and growth rate changes. The AI-2 response to glucose (a biphasic up-shift with an initial peak of more than fivefold and a second peak of ca. eightfold over initial AI-2 levels) and high osmolarity was consistent with those observed in earlier studies of *S. enterica* serovar Typhimurium (48), while the response to iron and DTT, to our knowledge, had not been previously shown. Similarly, iron exposure stimulated AI-2 activity more than threefold within the first 30 min. Contrarily, several stimuli (heat shock, ethanol, H_2O_2, serine hydroxamate, sodium acetate, hIL-2 overexpression, and oxygen) not only elicited a decrease in AI-2 activity but also increased degradation (or possibly inhibition). Of note, both heat and ethanol shock resulted in immediate down-regulation followed by highly reproducible oscillatory AI-2 responses, which, to our knowledge have not been previously reported. The observation that these two stimuli elicited similar AI-2 responses is not entirely surprising, as heat shock and ethanol shock exhibit overlapping responses, for example induction of the *psp* operon (7).

In general, however, the perturbations observed in Fig. 4 may not be specific to each individual stress, but more likely are indicative of a shift in the metabolic activity or state of the cells caused by the individual stress. We hypothesize that this change in metabolic state (physiologically seen as a change in growth rate but which may include other phenomena) was then responsible for changes in AI-2 signaling. In support of this notion, cells cultured entirely at a temperature of 42°C showed a constant higher level of AI-2 signal compared to cells grown entirely at 30°C. Importantly, this suggests cells cultured at a higher metabolic rate (i.e., higher growth rate) produce a higher level of AI-2 activity and corroborates results depicted in Fig. 1. Therefore, it is likely that the shift of metabolic state caused by the temperature upshift from 30 to 42°C was responsible for the perturbation in AI-2 seen in Fig. 4b. Further

TABLE 2. Steady-state ($\mu = 0.75\ h^{-1}$) AI-2 produced by mutant strains of *E. coli* at 30°C

Strain	Relevant characteristic or genotype	Specific fold AI-2 activity (s.s.)[a]	Source or reference
B178	W3110 *galE relA*	518	F. Baneyx
CG712	B178 *zjd*::Tn*10 groES30*	972	52
CG714	B178 *groEL140*	1,014	52
JZ12	B178 *zjd*::Tn*10 groES619 zje*::Kan^r	1,137	60
C600	F$^-$ *thi1 thr1 leuB6 lacY1 tonA21 supE44* λ^-	578	Laboratory stock
CG804	C600 *pheA*::Tn*10 grpE280*	442	3
MF746	C600 *dnaK756*	335	59
MF634	C600 *dnaJ259*	479	59

[a] Steady-state (s.s.) AI-2 activity level divided by OD_{600}. Fold activation represents the induction of luminescence (relative light units) in *V. harveyi* reporter strain BB170 (sensor 1$^-$sensor 2$^+$) from steady-state *E. coli* cultures grown in LB–50 mM glucose in relation to luminescence (relative light units) with fresh medium alone. Values are reported as the average of three independent activity measurements from three independent steady-state samples. OD_{600} of all cultures and replicate samples agreed within 10%.

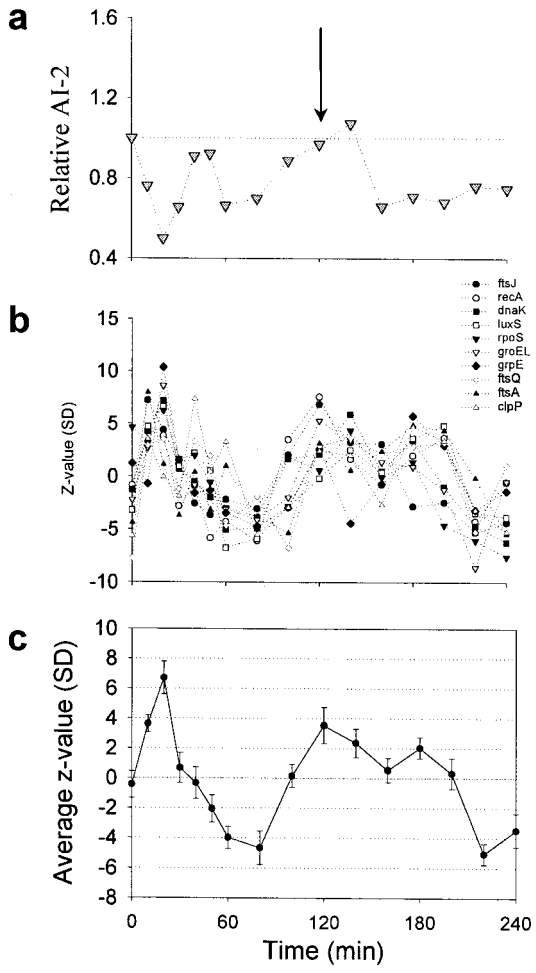

FIG. 7. Dynamic profile of highest correlated gene cluster during hIL-2 expression by steady-state W3110/phIL-2 cultures. Note, magnitude-independent *Z* values are reported. (a) AI-2 response to induction of hIL-2 expression with pulse addition of 1 mM IPTG at $t = 0$ and $t = 120$ min (black arrow). Seven genes clustered (correlation coefficient of 0.74) following induction of steady state-culture (b) and average *Z* value (mRNA response) of seven clustered genes (c). *Z* values were calculated as (sample − average)/standard deviation to allow examination of the dynamic changes in a variable independent of magnitude.

support of this idea is seen in the responses to sodium acetate, serine hydroxamate, and hIL-2 overexpression, in that all three stressors have been observed to decrease the metabolic activity and/or capacity of *E. coli* (11, 31, 42). Therefore, it was not entirely surprising that the production of AI-2 was observed to decrease relative to the steady-state level following each of these perturbations. Overall, these results demonstrate the utility of transient AI-2 profiling for comparative stimulus analysis, thereby elucidating future studies involving overlapping regulatory mechanisms.

Lastly, we attempted to correlate quorum-dependent transcriptional regulation with a subset of genes known to be upregulated in response to recombinant protein overexpression in batch culture (22). The transient transcriptional response of 24 genes, including four known quorum-related genes (*sdiA,* $luxS_{E.c.}$, *ftsQ*, and *ftsA*), to hIL-2 production, following an SOM-clustering reduction algorithm (15), resulted in 10 genes (*recA, rpoS, ftsJ, groEL, dnaK, grpE, clpP, luxS, ftsQ*, and *ftsA*) having highly significant statistical correlation ($r = 0.74$). The inclusion of *rpoS* in this cluster was not entirely surprising, as there is a growing body of evidence, including the presence of quorum and *rpoS*-regulated promoters upstream of *ftsQA* (44) and the induction of *rpoS* and *ftsQA* by homoserine lactone (29, 44), that *E. coli* may use quorum sensing as a signal to prepare for entry into stationary phase (reviewed in reference 35). Also, it is well-known that *dnaK, grpE, groEL*, and *recA* are all intimately involved in the folding of overexpressed heterologous proteins as well as the clearance of misfolded aggregates and premature polypeptides. Therefore, the similarity of responses among these genes, which includes four genes involved in the *E. coli* quorum circuit ($luxS_{E.c.}$, *sdiA, ftsQ*, and *ftsA*), suggests that autoinduction is intimately intertwined with the stress response to abnormal protein formation as well as other related stress responses (25). Consistent with these findings, both *recA* and *groEL*, which are similarly upregulated following hIL-2 expression, have been implicated in regulating *lux* expression in bioluminescent *E. coli* (53). Lastly, chemostat cultures of *groEL140, groES30*, and *groES619* and *dnak756, dnaJ259*, and *grpE280* further demonstrated the link between these stress-induced genes and AI-2 quorum signaling, as all produced altered levels (ca. 2-fold difference) of AI-2 quorum signal relative to those of their parent strain at 30°C. These results provide a direct link between AI-2 signaling and σ^{32}-mediated proteins, suggesting that a chaperone-mediated folding pathway exists that directly affects the accumulation of extracellular AI-2 under nominal growth conditions, similar to that proposed for bioluminescent *E. coli* (52).

Finally, it is well-known that environmental adaptation in *E. coli* involves increased rates of spontaneous mutation, shuffling or rearrangement of genomic content, and DNA methylation. We previously hypothesized that an adaptation of this nature was likely occurring during the transition to high cell density and during recombinant protein overexpression (20), and while this hypothesis was not specifically tested here, the dissimilar responses observed following the initial and subsequent pulse addition of IPTG is likely indicative of culture adaptation to heterologous protein formation. Similar adaptation, consistent with this result, has been demonstrated for glucose uptake and protease up-regulation in response to two consecutive pulses inducing recombinant protein expression (27).

Importantly, quorum sensing in gram-negative bacteria is an excellent example of how individual prokaryotic cells transduce physiologically based signals into coordinated, multigenic responses. An emerging blueprint holds that the *E. coli* quorum circuit is regulated by a complex, overlapping network built upon a distinct autoinducer molecule (AI-2), synthesized by LuxS (homologous to *V. harveyi* LuxS), and used to channel environmental information to a response regulator protein, SdiA (homologous to *V. fischeri* LuxR), for density-dependent control of gene expression. We have demonstrated that studying the transients in chemostat culture has improved our knowledge of global regulation of AI-2 in the prevailing bioreactor environment, where the effect of transients, such as physical and/or chemical gradients, on overall cell and/or heterologous protein productivity are poorly defined. Understanding the role of cell-to-cell signaling in complex environ-

ments (e.g., high density, low oxygen solubility, substrate and nutrient gradients or limitations, evolution of excess metabolic heat, and overflow metabolism) common among numerous manufacturing bioprocesses may begin to explain attenuated productivity as well as many other physiological changes (i.e., cell morphology, increased lysis rates, reduced metabolic activity rates, and decreased reproductive viability) that occur as cells progress to higher densities rarely seen in the natural environment.

ACKNOWLEDGMENTS

We thank B. Bassler, P. Dunlap, and F. Baneyx for generously providing strains used in this study.

This research was supported by the U.S. Army Engineering Research and Development Center, Edgewood, Md. (grant DAAM01-96-0037).

REFERENCES

1. **Adar, Y. Y., M. Simaan, and S. Ulitzur.** 1992. Formation of the LuxR protein in the *Vibrio fischeri lux* system is controlled by HtpR through the GroESL proteins. J. Bacteriol. **174:**7138–7143.
2. **Andersson, L., S. Yang, P. Neubauer, and S. O. Enfors.** 1996. Impact of plasmid presence and induction on cellular responses in fed batch cultures of *Escherichia coli*. J. Biotechnol. **46:**255–263.
3. **Ang, D., and C. Georgopoulos.** 1989. The heat-shock-regulated *grpE* gene of *Escherichia coli* is required for bacterial growth at all temperatures but is dispensable in certain mutant backgrounds. J. Bacteriol. **171:**2748–2755.
4. **Baca-DeLancey, R. R., M. M. South, X. Ding, and P. N. Rather.** 1999. *Escherichia coli* genes regulated by cell-to-cell signaling. Proc. Natl. Acad. Sci. USA **96:**4610–4614.
5. **Bainton, N. J., P. Stead, S. R. Chhabra, B. W. Bycroft, G. P. Salmond, G. S. Stewart, and P. Williams.** 1992. *N*-(3-Oxohexanoyl)-L-homoserine lactone regulates carbapenem antibiotic production in *Erwinia carotovora*. Biochem. J. **288:**997–1004.
6. **Bassler, B. L., M. Wright, and M. R. Silverman.** 1994. Multiple signalling systems controlling expression of luminescence in *Vibrio harveyi*: sequence and function of genes encoding a second sensory pathway. Mol. Microbiol. **13:**273–286.
7. **Brissette, J. L., L. Weiner, T. L. Ripmaster, and P. Model.** 1991. Characterization and sequence of the *Escherichia coli* stress-induced *psp* operon. J. Mol. Biol. **220:**35–48.
8. **Cha, H. J., R. Srivastava, V. N. Vakharia, G. Rao, and W. E. Bentley.** 1999. Green fluorescent protein as a noninvasive stress probe in resting *Escherichia coli* cells. Appl. Environ. Microbiol. **65:**409–414.
9. **Cha, H. J., C. F. Wu, J. J. Valdes, G. Rao, and W. E. Bentley.** 2000. Observations of green fluorescent protein as a fusion partner in genetically engineered *Escherichia coli*: monitoring protein expression and solubility. Biotechnol. Bioeng. **67:**565–574.
10. **Chu, S., J. DeRisi, M. Eisen, J. Mulholland, D. Botstein, P. O. Brown, and I. Herskowitz.** 1998. The transcriptional program of sporulation in budding yeast. Science **282:**699–705.
11. **DeLisa, M. P., J. Li, G. Rao, W. A. Weigand, and W. E. Bentley.** 1999. Monitoring GFP-operon fusion protein expression during high cell density cultivation of *Escherichia coli* using an on-line optical sensor. Biotechnol. Bioeng. **65:**54–64.
12. **Dolan, K. M., and E. P. Greenberg.** 1992. Evidence that GroEL, not sigma 32, is involved in transcriptional regulation of the *Vibrio fischeri* luminescence genes in *Escherichia coli*. J. Bacteriol. **174:**5132–5135.
13. **Dunlap, P. V.** 1992. Iron control of the *Vibrio fischeri* luminescence system in *Escherichia coli*. Arch. Microbiol. **157:**235–241.
14. **Dunlap, P. V., and E. P. Greenberg** 1985. Control of *Vibrio fischeri* luminescence gene expression in *Escherichia coli* by cyclic AMP and cyclic AMP receptor protein. J. Bacteriol. **164:**45–50.
15. **Eisen, M. B., P. T. Spellman, P. O. Brown, and D. Botstein.** 1998. Cluster analysis and display of genome-wide expression patterns. Proc. Natl. Acad. Sci. USA **95:**14863–14868.
16. **Everitt, B., and G. Dunn.** 1991. Applied multivariate data analysis. John Wiley and Sons, Inc., New York, N.Y.
17. **Freeman, J. A., and B. L. Bassler.** 1999. A genetic analysis of the function of LuxO, a two-component response regulator involved in quorum sensing in *Vibrio harveyi*. Mol. Microbiol. **31:**665–677.
18. **Garcia-Lara, J., L. H. Shang, and L. I. Rothfield.** 1996. An extracellular factor regulates expression of *sdiA*, a transcriptional activator of cell division genes in *Escherichia coli*. J. Bacteriol. **178:**2742–2748.
19. **Georgiou, G.** 1988. Optimizing the production of recombinant proteins in microorganisms. AIChEJ **34:**1233–1248.
20. **Gill, R., M. DeLisa, J. Valdes, and W. Bentley.** 2000. Genomic analysis of high-cell-density recombinant *Escherichia coli* fermentation and "cell conditioning" for improved recombinant protein yield. Biotechnol. Bioeng. **72:**85–95.
21. **Gill, R. T., H. J. Cha, A. Jain, G. Rao, and W. E. Bentley.** 1998. Generating controlled reducing environments in aerobic recombinant *Escherichia coli* fermentations: effects on cell growth, oxygen uptake, heat shock protein expression, and *in vivo* CAT activity. Biotechnol. Bioeng. **59:**248–259.
22. **Gill, R. T., J. J. Valdes, and W. E. Bentley.** 2000. A comparative study of global stress gene regulation in response to overexpression of recombinant proteins in *Escherichia coli*. Metabol. Eng. **2:**178–189.
23. **Gill, R. T., J. J. Valdes, and W. E. Bentley.** 1999. RT-PCR differential display analysis of *Escherichia coli* global gene regulation in response to heat shock. Appl. Environ. Microbiol. **65:**5386–5393.
24. **Glick, B.** 1995. Metabolic load and heterologous gene expression. Biotechnol. Adv. **13:**247–261.
25. **Goff, S. A., and A. L. Goldberg.** 1985. Production of abnormal proteins in *E. coli* stimulates transcription of *lon* and other heat shock genes. Cell **41:**587–595.
26. **Greenberg, E. P., J. W. Hastings, and S. Ulitzur.** 1979. Induction of luciferase synthesis in *Beneckea harveyi* by other marine bacteria. Arch. Microbiol. **120:**87–91.
27. **Harcum, S. W., and W. E. Bentley.** 1993. Response dynamics of 26-, 34-, 39-, 54-, and 80-kDa proteases in induced cultures of recombinant *Escherichia coli*. Biotechnol. Bioeng. **42:**675–685.
28. **Hewitt, C. J., G. Nebe-Von Caron, A. W. Nienow, and C. M. McFarlane.** 1999. Use of multi-staining flow cytometry to characterise the physiological state of *Escherichia coli* W3110 in high cell density fed-batch cultures. Biotechnol. Bioeng. **63:**705–711.
29. **Huisman, G. W., and R. Kolter.** 1994. Sensing starvation: a homoserine lactone-dependent signaling pathway in *Escherichia coli*. Science **265:**537–539.
30. **Huisman, O., R. D'Ari, and S. Gottesman.** 1984. Cell-division control in *Escherichia coli*: specific induction of the SOS function SfiA protein is sufficient to block septation. Proc. Natl. Acad. Sci. USA **81:**4490–4494.
31. **Jensen, E. B., and S. Carlsen.** 1990. Production of recombinant human growth hormone in *Escherichia coli*: expression of different precursors and physiological effects of glucose, acetate, and salts. Biotechnol. Bioeng. **36:**1–11.
32. **Kanamaru, K., I. Tatsuno, T. Tobe, and C. Sasakawa.** 2000. SdiA, an *Escherichia coli* homologue of quorum-sensing regulators, controls the expression of virulence factors in enterohaemorrhagic *Escherichia coli* O157:H7. Mol. Microbiol. **38:**805–816.
33. **Kanemori, M., H. Mori, and T. Yura.** 1994. Induction of heat shock proteins by abnormal proteins results from stabilization and not increased synthesis of sigma 32 in *Escherichia coli*. J. Bacteriol. **176:**5648–5653.
34. **Latifi, A., M. K. Winson, M. Foglino, B. W. Bycroft, G. S. Stewart, A. Lazdunski, and P. Williams.** 1995. Multiple homologues of LuxR and LuxI control expression of virulence determinants and secondary metabolites through quorum sensing in *Pseudomonas aeruginosa* PAO1. Mol. Microbiol. **17:**333–343.
35. **Lazazzera, B. A.** 2000. Quorum sensing and starvation: signals for entry into stationary phase. Curr. Opin. Microbiol. **3:**177–182.
36. **Lee, S. Y.** 1996. High cell-density culture of *Escherichia coli*. Trends Biotechnol. **14:**98–105.
37. **Nealson, K. H.** 1999. Early observations defining quorum-dependent gene expression, p. 277–289. *In* G. M. Dunny and S. C. Winans (ed.), Cell-cell signaling in bacteria. ASM Press, Washington, D.C.
38. **Nealson, K. H., A. Eberhard, and J. W. Hastings.** 1972. Catabolite repression of bacterial bioluminescence: functional implications. Proc. Natl. Acad. Sci. USA **69:**1073–1076.
39. **Nealson, K. H., T. Platt, and J. W. Hastings.** 1970. Cellular control of the synthesis and activity of the bacterial luminescent system. J. Bacteriol. **104:**313–322.
40. **Piper, K. R., S. Beck von Bodman, and S. K. Farrand.** 1993. Conjugation factor of *Agrobacterium tumefaciens* regulates Ti plasmid transfer by autoinduction. Nature **362:**448–450.
41. **Pirt, S. J.** 1975. Principles of microbe and cell cultivation. Blackwell Scientific Publications, Oxford, England.
42. **Pizer, L. I., and J. P. Merlie.** 1973. Effect of serine hydroxamate on phospholipid synthesis in *Escherichia coli*. J. Bacteriol. **114:**980–987.
43. **Schweder, T., E. Kruger, B. Xu, B. Jurgen, G. Blomsten, S. O. Enfors, and M. Hecker.** 1999. Monitoring of genes that respond to process-related stress in large-scale bioprocesses. Biotechnol. Bioeng. **65:**151–159.
44. **Sitnikov, D. M., J. B. Schineller, and T. O. Baldwin.** 1996. Control of cell division in *Escherichia coli*: regulation of transcription of *ftsQA* involves both *rpoS* and SdiA-mediated autoinduction. Proc. Natl. Acad. Sci. USA **93:**336–341.
45. **Sitnikov, D. M., J. B. Schineller, and T. O. Baldwin.** 1995. Transcriptional regulation of bioluminescence genes from *Vibrio fischeri*. Mol. Microbiol. **17:**801–812.
46. **Sperandio, V., J. L. Mellies, W. Nguyen, S. Shin, and J. B. Kaper.** 1999.

Quorum sensing controls expression of the type III secretion gene transcription and protein secretion in enterohemorrhagic and enteropathogenic *Escherichia coli*. Proc. Natl. Acad. Sci. USA **96:**15196–15201.
47. **Surette, M. G., and B. L. Bassler.** 1998. Quorum sensing in *Escherichia coli* and *Salmonella typhimurium*. Proc. Natl. Acad. Sci. USA **95:**7046–7050.
48. **Surette, M. G., and B. L. Bassler.** 1999. Regulation of autoinducer production in *Salmonella typhimurium*. Mol. Microbiol. **31:**585–595.
49. **Surette, M. G., M. B. Miller, and B. L. Bassler.** 1999. Quorum sensing in *Escherichia coli, Salmonella typhimurium*, and *Vibrio harveyi*: a new family of genes responsible for autoinducer production. Proc. Natl. Acad. Sci. USA **96:**1639–1644.
50. **Swartz, J. R.** 1996. *Escherichia coli* recombinant DNA technology, p. 1693–1711. *In* F. C. Neidhardt, R. Curtiss, J. L. Ingraham, E. C. C. Lin, K. B. Low, B. Magasanik, W. S. Reznikoff, M. Riley, M. Schaechter, and H. E. Umbarger (ed.), *Escherichia coli* and *Salmonella*, 2nd ed. vol. 2. ASM Press, Washington, D.C.
51. **Taylor, J.** 1982. An introduction to error analysis. University Science Books, Mill Valley, Calif.
52. **Tilly, K., N. McKittrick, C. Georgopoulos, and H. Murialdo.** 1981. Studies on *Escherichia coli* mutants which block bacteriophage morphogenesis. Prog. Clin. Biol. Res. **64:**35–45.
53. **Ulitzer, S., and P. V. Dunlap.** 1995. Regulatory circuitry controlling luminescence autoinduction in *Vibrio fischeri*. Photochem. Photobiol. **62:**625–632.
54. **VanBogelen, R. A., P. M. Kelley, and F. C. Neidhardt.** 1987. Differential induction of heat shock, SOS, and oxidation stress regulons and accumulation of nucleotides in *Escherichia coli*. J. Bacteriol. **169:**26–32.
55. **Van Dyk, T. K., T. R. Reed, A. C. Vollmer, and R. A. LaRossa.** 1995. Synergistic induction of the heat shock response in *Escherichia coli* by simultaneous treatment with chemical inducers. J. Bacteriol. **177:**6001–6004.
56. **Wang, M. Y., and W. E. Bentley.** 1994. Continuous insect cell (Sf-9) culture with aeration through sparging. Appl. Microbiol. Biotechnol. **41:**317–323.
57. **Wang, X. D., P. A. de Boer, and L. I. Rothfield.** 1991. A factor that positively regulates cell division by activating transcription of the major cluster of essential cell division genes of *Escherichia coli*. EMBO J. **10:**3363–3372.
58. **Withers, H. L., and K. Nordstrom.** 1998. Quorum-sensing acts at initiation of chromosomal replication in *Escherichia coli*. Proc. Natl. Acad. Sci. USA **95:**15694–15699.
59. **Yochem, J., H. Uchida, M. Sunshine, H. Saito, C. P. Georgopoulos, and M. Feiss.** 1978. Genetic analysis of two genes, *dnaJ* and *dnaK*, necessary for *Escherichia coli* and bacteriophage lambda DNA replication. Mol. Gen. Genet. **164:**9–14.
60. **Zeilstra-Ryalls, J., O. Fayet, L. Baird, and C. Georgopoulos.** 1993. Sequence analysis and phenotypic characterization of *groEL* mutations that block lambda and T4 bacteriophage growth. J. Bacteriol. **175:**1134–1143.